 https://doi.org/10.3311/PPch.22043

Periodica Polytechnica Chemical Engineering, 67(3), pp. 504–515, 2023

Cellulose, Cellulose Benzoate and Cellulose Citrate from Screw Pine (*Pandanus tectorius*) Leaves as PVDF Filler for Improved Permeability and Anti-fouling Properties

Elyna Wahyu Trisnawati[1], Indri Sri Cahyani[1], Diah Safriyani[1], Edi Pramono[1], Venty Suryanti[1*]

[1] Department of Chemistry, Faculty of Mathematics and Natural Sciences, Universitas Sebelas Maret, Jl. Ir. Sutami 36A, 57126 Surakarta, Indonesia
[*] Corresponding author, e-mail: venty@mipa.uns.ac.id

Received: 12 February 2023, Accepted: 01 June 2023, Published online: 10 July 2023

Abstract

Cellulose was isolated from screw pine (*Pandanus tectorius*) leaves through an alkalization and bleaching process and synthesized into cellulose benzoate and cellulose citrate. Cellulose, cellulose benzoate, and cellulose citrate were introduced to polyvinylidene fluoride (PVDF) matrix as fillers via blending-phase inversion method to improve PVDF membrane permeability and anti-fouling properties. The effect of cellulose, cellulose benzoate, and cellulose citrate fillers on PVDF membrane hydrophilicity, permeability, selectivity, anti-fouling properties, and morphology was investigated. The result demonstrates that the PVDF membrane's hydrophilicity, permeability, and anti-fouling properties were improved by the addition of filler. With the addition of 0.3% of cellulose, cellulose citrate, and cellulose benzoate, water permeability in PVDF was doubled. PVDF membrane rejection of methylene blue increased up to 86, 85 and 82%, respectively, with the addition of 0.3% cellulose, cellulose citrate, and cellulose benzoate. Anti-fouling properties value increased up to 89% in 0.3% cellulose citrate addition. These results indicated that cellulose, cellulose benzoate, and cellulose citrate from screw pine leaves are excellent for PVDF membrane fillers which are comparable with other reported membranes.

Keywords

anti-fouling, cellulose, cellulose benzoate, cellulose citrate, polyvinylidene fluoride

1 Introduction

Polyvinylidene fluoride (PVDF) is a semi-crystalline polymer with a crystalline and amorphous phase. PVDF is the material used in membrane the most due to its high mechanical strength, thermal stability, chemical resistance, and simplicity of fabrication [1]. Membrane is typically favored because of its inherent benefits, including its low cost, ease of use, high recovery rate, high level of selectivity, low pollution, and ability to work in conjunction with other wastewater treatment methods [2–4]. PVDF membrane has been widely used in water treatment, microfiltration, ultrafiltration, and distillation [5]. However, PVDF membrane has limitation due to their hydrophobic properties that reduce membrane performances such as water permeability, rejection, and fouling resistance [2]. Hence, hydrophilic modification is proposed to increase PVDF membrane performances and lifetimes that have growing interest in recent years membrane technology [6, 7].

The performance of the membrane is enhanced by raising its hydrophilicity. Several techniques are utilized to enhance membrane performance, including surface grafting or coating, chemical modification, and mixing alteration. Modification by blending with hydrophilic polymers, such as cellulose and its derivatives, is the easiest and most widely used strategy to alter membrane structure [5, 6]. Cellulose has a large specific surface area, low density, and high porosity which is made up of anhydroglucose units connected by β-1,4-glycosidic bonds [8, 9]. Cellulose has been isolated from a variety of plant parts, such as cocoa pod husk [10], banana stem [11], groundnut shells [12], sugarcane bagasse [13], coccinia grandis stem [14] and screw pine leaves (*Pandanus tectorius*) [15, 16]. There has been relatively little research carried out on cellulose of screw pine leaves. Screw pine leaves contains 37.30% cellulose, 34.40% hemicellulose, 24.00% lignin, and 2.5% extractive content [16]. Screw pine leaves are widely used for making rope, weddings, basket, chairs, weaving hats and mats [15, 16].

Three hydroxyl groups of cellulose can be modified by adding specific functional groups for obtaining cellulose

Cite this article as: Trisnawati E. W., Cahyani, I. S., Safriyani, D., Pramono, E., Suryanti, V. "Cellulose, Cellulose Benzoate and Cellulose Citrate from Screw Pine (*Pandanus tectorius*) Leaves as PVDF Filler for Improved Permeability and Anti-fouling Properties", Periodica Polytechnica Chemical Engineering, 67(3), pp. 504–515, 2023. https://doi.org/10.3311/PPch.22043

derivatives. Modification of cellulose can improve its properties which increases the variety of uses for it in areas including biomedicine, agriculture, water purification and food industry [8]. Cellulose esters have many advantages such as biodegradable, low-cost, non-toxic, and heat resistant [17, 18]. The use of cellulose and cellulose acetate in membrane technology has increased recently [7, 19–21]. Adding cellulose to PVDF matrix can enhance the hydrophilicity and anti-fouling qualities of the membrane. Addition 0.5 and 1% cellulose improve hydrophilicity, water permeability, rejection, and Flux Recovery Ratio (FRR) value of PVDF membrane [21]. In membrane technology, cellulose acetate (CA) is frequently utilized as matrix membranes or PVDF membrane filler [19, 22–25].

Other cellulose derivatives, such as cellulose benzoate (CB) and cellulose citrate (CC) have been studied. CB is most frequently employed in separation enantiomer [26, 27], while CC is widely used in adsorption fields and bio-composite materials [28–30]. CB and CC have never been applied as fillers in PVDF membranes. CB and CC are expected to have better properties than that of CA for improving PVDF membrane performances, because their structure has hydrophilic groups that can increase hydrophilicity, thereby increasing the permeability and anti-fouling properties of PVDF membranes.

The aim of this study was to evaluate the effect of CB, CC and screw pine leave cellulose as PVDF membrane filler which was fabricated by phase inversion method and followed by assessing membrane performances on hydrophilicity, water permeability, selectivity, anti-fouling properties, and morphology. In this work, cellulose was isolated from screw pine leaves and synthesized into CB and CC by esterification.

2 Materials and methods

2.1 Materials

Screw pine leaves (SP) was collected from Yogyakarta coastal area, Indonesia. Natrium hydroxide, natrium hypochlorite, pyridine, benzoyl chloride, citric acid, dimethylacetamide, polyethylene glycol (PEG) Mw 400 Da as pore-former were purchased from E-merck. Poly(vinylidene Fluoride) (Solef PVDF 1010 Mw 352 kDa) was obtained from Solvay.

2.2 Instrumentations

FTIR analysis was carried out on an IR Prestige-21 SHIMADZU spectroscopy. TGA analysis was conducted by Linseis PT – 1600 thermogravimetric analyzer. SEM analysis of membranes were performed using JEOL Benchtop JCM 7000. ATR-FTIR was analyzed by Carry 630 Agilent in the range 650–4000 cm^{-1}.

2.3 Methods

2.3.1 Isolation of cellulose

Preparation and isolation cellulose from SP refer to [16] and [31]. SP were washed with water and dried sun. Dried SP were grounded and sieved. SP powder was added NaOH 10% (1:20, w/v), stirred at 80 °C for 2 h, and then neutralized with water. The slurry was added NaOCl 4% (1:20, w/v) pH 4.5, stirred at 80 °C for 2 h. The mixture was neutralization with water and dried to obtaine screw pine leaves cellulose (SPC) which was analyzed by fourier-transform infrared spectroscopy (FT-IR) and thermogravimetric analysis (TGA).

2.3.2 Synthesis of cellulose benzoate and cellulose citrate

Cellulose benzoate was synthesized following Zhang et al. method [32]. SPC (0.5 g) was added with 25 mL pyridine and stirred at 40 °C for 30 mins. Then, the mixture was added with 10 mL benzoyl chloride and stirred at 50 °C for 3 h. At last, acetone was added to the mixture, stirred for 1 h, and then filtered. The precipitation was washed with water and dried to obtain cellulose benzoate (SPCB).

Cellulose citrate was synthesised following to Solo et al. method [33]. Firstly, a citric acid solution was obtained by dissolving of 3.5 g citric acid in 5 mL distilled water. Citric acid solution was then added 0.5 g SPC, stirred for 2 h and transferred to an evaporating dish. The mixture was put in the oven at 50 °C for 24 h and further heated 90 °C for 90 mins, then leaved to cool. Secondly, the slurry was added with 10 mL distilled water, stirred for 1 h. The solution is neutralized and dried to obtain cellulose citrate (SPCC). The synthesized cellulose benzoate and cellulose citrate were analyzed by FTIR and TGA.

2.3.3 Fabrication of PVDF/SPC, PVDF/SPCB, and PVDF/SPCC Membranes

PVDF/SPC, PVDF/SPCB, and PVDF/SPCC membranes were fabricated using phase inversion method [21]. Dope solution was produced using blending method. Firstly, dimethylacetamide (DMAc) and PEG 400 were stirred for 5 mins. The mixture was added with filler (SPC, SPCB or SPCC) and stirred for 10 mins. PVDF was added last and the dope solution was stirred for 24 h at 60 °C. The dope solution was cast in a glass plate and immersed in coagulant

bath containing distilled water. The formed membrane was stored in glycerin for further analysis. The scheme of fabrication membranes was shown in Fig. 1.

Membranes from glycerin storage was washed with distilled water before analysis. Top surface and cross-section of membrane were analyzed using scanning electron microscope (SEM). Attenuated total reflection-Fourier transform infrared spectroscopy (ATR-FTIR) was used to analyze functional groups in membrane surface. Thermal stability of membrane was analyzed by TGA. PVDF membrane was modified with filler (SPC, SPCB and SPCC). The composition of filler in the dope solution was shown in Table 1.

2.3.4 Analysis of PVDF/SPC, PVDF/SPCB, and PVDF/SPCC membrane performance

Membrane performance analysis was evaluated by water permeability from pure water flux (PWF) and water flux, rejection, and FRR which was continuously measured using dead-end system. PWF was measurement carried out by placed membrane with 5 cm diameter in a stirred cell and filled with distilled water. The diameter is used to calculate the surface area of membrane (A). Rejection and water flux test were conducted with replaced the distilled water with 100 ppm methylene blue (MB) solution. FRR test was carried out by replacing the MB solution with a small amount of distilled water to wash the surface membrane, then was filled with new distilled water. System compaction was performed at 2 bars for 15 mins before every measurement. The amount of permeate volume (v) was collected and the operating time used (t) was calculated.

2.4 Characterization procedures

Samples were analyzed with KBr plate in the range 500–4000 cm^{-1}. Samples for TGA analysis were heated from 30 to 900 °C with a heating rate 10 °C per min at atmospheric conditions. Membranes were broken in liquid nitrogen and gold coated for 5 min before SEM analysis. ATR-FTIR in the range 650–4000 cm^{-1}.

Cellulose chain has three OH groups per anhydroglucose (AGU) unit [34]. The percentage of OH groups can be determined from the degree of substitution (DS) per AGU after the esterification process on cellulose benzoate and

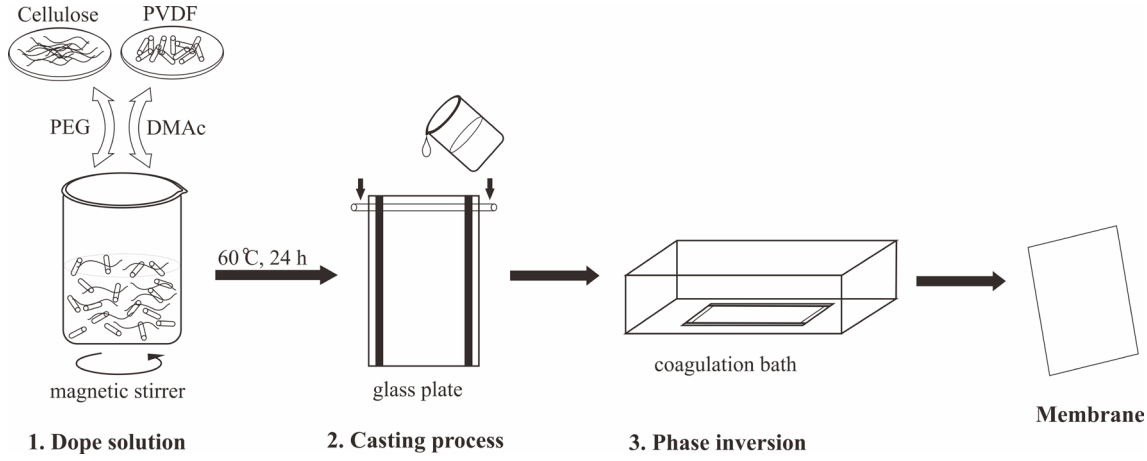

Fig. 1 Scheme of fabrication membranes

Table 1 Composition of fillers in the dope solution

Membranes	Composition (% w/w)					
	PVDF (%)	PEG 400 (%)	DMAc (%)	Fillers (%)		
				SPC	SPCB	SPCC
PM	18	4	78.00	–	–	–
PMC0.1	18	4	77.90	0.10	–	–
PMC0.3	18	4	77.70	0.30	–	–
PMC0.5	18	4	77.50	0.50	–	–
PMC1	18	4	77.00	1.00	–	–
PMC1.5	18	4	76.50	1.50	–	–
PMCB0.3	18	4	77.70	–	0.30	–
PMCC0.3	18	4	77.70	–	–	0.30

cellulose citrate. DS can be calculated using absorbance (Abs) C=O esters at ~1730 cm^{-1} and Abs C-O cellulose at ~1060 cm^{-1} in Eq. (1) [35]:

$$\mathrm{DS} = \frac{\mathrm{Abs}_{\mathrm{C=Oesters}}}{\mathrm{Abs}_{\mathrm{C-Ocellulose}}}. \quad (1)$$

Membrane characterization was determined by water contact angle, porosity, average pore size, and beta fraction. Membrane porosity (ε) and average pore size (r) were evaluated using gravimetric method and Guerout–Elford–Ferry equation, respectively [24]. The wet (W_{wet}) and dried (W_{dried}) membranes which were heated at 60 °C for 24 h were weighed. The thickness of wet membranes (I_{wet}) was measured and is water density ($g\ cm^{-3}$). Membrane porosity is calculated by Eq. (2) and membrane average pore size is measured by Eq. (3):

$$\varepsilon(\%) = \left(\frac{W_{\mathrm{wet}} - W_{\mathrm{dried}}}{A \times I_{\mathrm{wet}} \times \rho}\right), \quad (2)$$

$$r = \sqrt{\frac{(2.9 - 1.75\varepsilon) \times 8\eta l_m J_1}{3800 \times \varepsilon \times \Delta P}}, \quad (3)$$

where ε is the porosity (%), ΔP is pressure (Pa), η is viscosity of water at 25 °C (8.9×10^{-4} Pa s), l_m is wet thickness of the membrane (m), A is the membrane area (m^2) and J_1 is pure water flux (PWF) ($L\ m^{-2}\ h^{-1}$). The value of PWF (J_1) and water flux (J_2) is determined by Eq. (4), rejection value (R) is determined by Eq. (5) which concentration of permeate (C_p) and retentate (C_r) were measured by UV-Vis spectroscopy (HITACHI UH5300) at 664 nm, and FRR value is determined by Eq. (6) [6]:

$$J_1 = \frac{v}{A \times t}, \quad (4)$$

$$\%R = \left(1 - \frac{C_p}{C_r}\right) \times 100\%, \quad (5)$$

$$\mathrm{FRR} = \frac{J_2}{J_1} \times 100\%. \quad (6)$$

3 Results and discussion

3.1 Synthesis of cellulose benzoate and cellulose citrate

FT-IR spectra and thermogram of cellulose correspond with the previous study [16]. Removal of hemicellulose and lignin from cellulose was confirmed by the absence of the carbonyl group in the SPC FTIR spectra. SPC is used as a starting material for synthesizing of SPCB and SPCC. FT-IR spectra and thermogram of SPC, SPCB, and SPCC are shown in Fig. 2.

FT-IR spectra of SPCB in Fig. 2 (a) shows new peaks at 3065 cm^{-1} for C-H of benzene ring, 1729 cm^{-1} for C=O ester, 1601 cm^{-1}, and 1451 cm^{-1} for C=C benzene ring, 1270 cm^{-1} for C-O carboxylate, and 709 cm^{-1} for mono-substituted C-H benzene group. Benzoylation process decreased a peak at 3416 cm^{-1}, indicating substitution of hydroxyl groups [27, 32]. SPCC spectra showed appearance of a new peak at 1730 cm^{-1} for C=O carbonyl ester and decreasing a peak intensity of 3411 cm^{-1}, indicating substitution hydroxyl group with citrate functional group [30, 36]. The FTIR spectra confirmed that SPCB and SPCC were successfully synthesized by non-Fischer reaction. The DS value of cellulose benzoate is 0.1 and cellulose citrate is 0.2. Thus the OH group substituted on cellulose benzoate is 3.33% and cellulose citrate is 6.67% per AGU. Whereas, the OH group present on cellulose benzoate is 96.67% and cellulose citrate is 106.67%, because every 1 g/mol of citric acid has three OH groups.

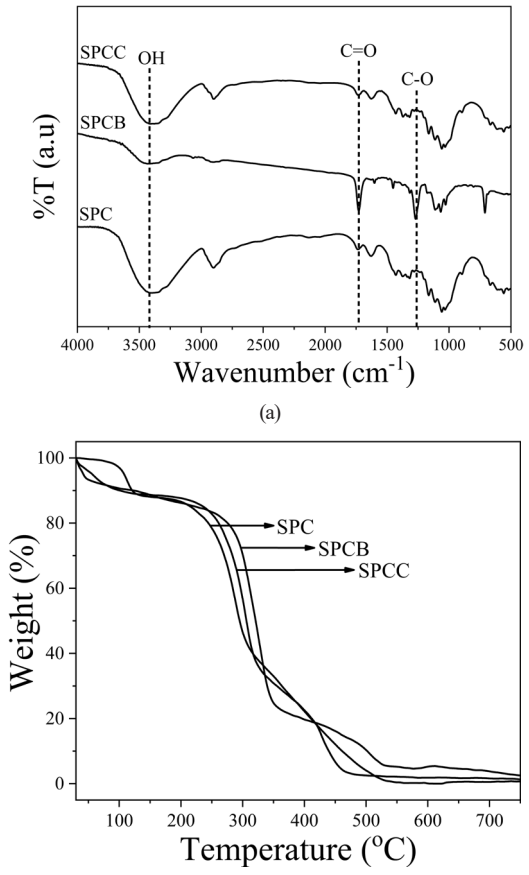

Fig. 2 FTIR spectra (a) and thermogram (b) of SPC, SPCB, and SPCC

Thermal stability of SPC was improved by the esterification process (Fig. 2 (b)), where higher degradation temperatures of SPCB and SPCC were occurred [37]. Because a large amount of water in SPC is bounded by hydroxyl groups, weight decrease was greater at the early stage of degradation [38]. Degradation of the SPCB and SPCC polymer chain was occurred at second stage, and the decarbonization stage form CO_2 gas was took place at third stage [13, 39]. SPC, SPCB, and SPCC have thermal stability at the second stage of 200, 270, and 250 °C, respectively. Higher thermal stability of SPCB and SPCC than SPC due to substitution of hydroxyl groups with C=O carbonyl ester groups.

3.2 PVDF/SPC membrane

For initial study, PVDF/SPC membranes were fabricated using variation concentration of SPC as shown in Table 1. Membrane performances were investigated for porosity and average pore size (Fig. 3 (a)). PMC0.3 membrane shows the highest value of porosity and average pore size since hydroxyl groups of cellulose enhanced the diffusional exchange rate of solvent and non-solvent, resulting in large pores [40]. The water contact angle was measured to determine the membrane surface hydrophilicity. The water contact angle of PVDF/SPC membranes decreased with the increase of cellulose addition (Fig. 3 (b)). During phase inversion process, cellulose migrated to membrane surface due to its high affinity with water, then generated smooth skin layer which can improve hydrophilicity of PVDF/cellulose membranes [41]. The highest standard deviation (SD) obtained for all parameters examined was 4.82 in PMC0.3, indicating strong homogeneity (SD < 5%). Cellulose addition increased average pore size and lowered water contact angle significantly ($p < 0.05$) but raised PVDF membrane porosity insignificantly ($p > 0.05$).

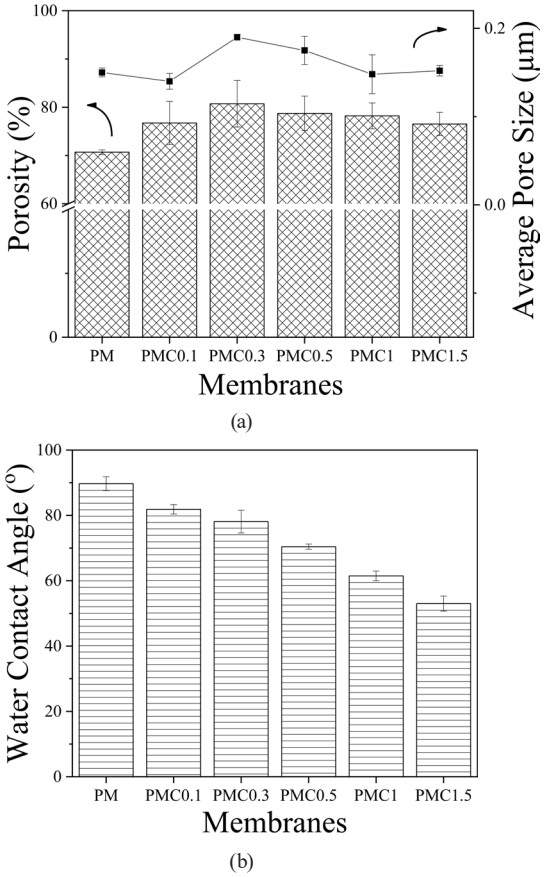

Fig. 3 Porosity and average pore size (a), water contact angle (b) of PVDF and PVDF/SPC membranes

All PVDF/SPC membranes, excluded PMC0.1, gave increasing pure water flux (PWF) value after the addition of cellulose (Fig. 4 (a)). When 0.3% w/w cellulose was added to the PVDF membrane, the double PWF value increased from 17.08 to 36.85 L m^{-2} h^{-1}. Increased hydrophilicity and improved pore size, which allow water molecules to move across membranes with ease, were credited with increasing PWF value [2, 42, 43]. In this study, adding 0.3% w/w of cellulose generated membrane with the highest pure water flux, porosity and pore size. The membrane with the smallest pore size was PMC0.1 which has the lowest PWF value.

Upon addition up to 0.3% w/w of cellulose, MB rejection and water flux of the membranes declined, while increasing amount of cellulose addition resulted in decreasing MB rejection and water flux of the membranes (Fig. 4 (b)). The rejection value of the PVDF membrane increased from 82.89% to 86.50%, due to the hydrogen bond formed by hydroxyl group of the surface membrane and $-NH_2$ group of the MB [44]. The PVDF membrane's water flux value increased doubled, from 11.22 to 23.49 L m^{-2} h^{-1}. Water could pass through the membrane more quickly with 0.3% w/w cellulose added due to its high porosity and pore size [45]. Water flux was reduced by the addition of more than 0.3% w/w of cellulose because porosity and pore size decreased [46].

The highest FRR value of 88.29% was obtained for PMC 1.5 (Fig. 4 (c)), which is the greatest hydrophilic membrane. Because hydroxyl groups of cellulose created a hydration layer on the surface of the membrane and reduced dye blocking and hydrophobic interactions between membrane and MB [47]. FRR of PMC0.3 and PMC0.5 decreased from 80.26% to 74.96% and 76.38%, respectively. Poor dispersion of filler particles [48], large porosity and pore size of PMC0.3 and PMC0.5 resulted pore blocking by MB molecules which could not be removed by washing treatment [40]. The largest standard deviation (SD) recorded

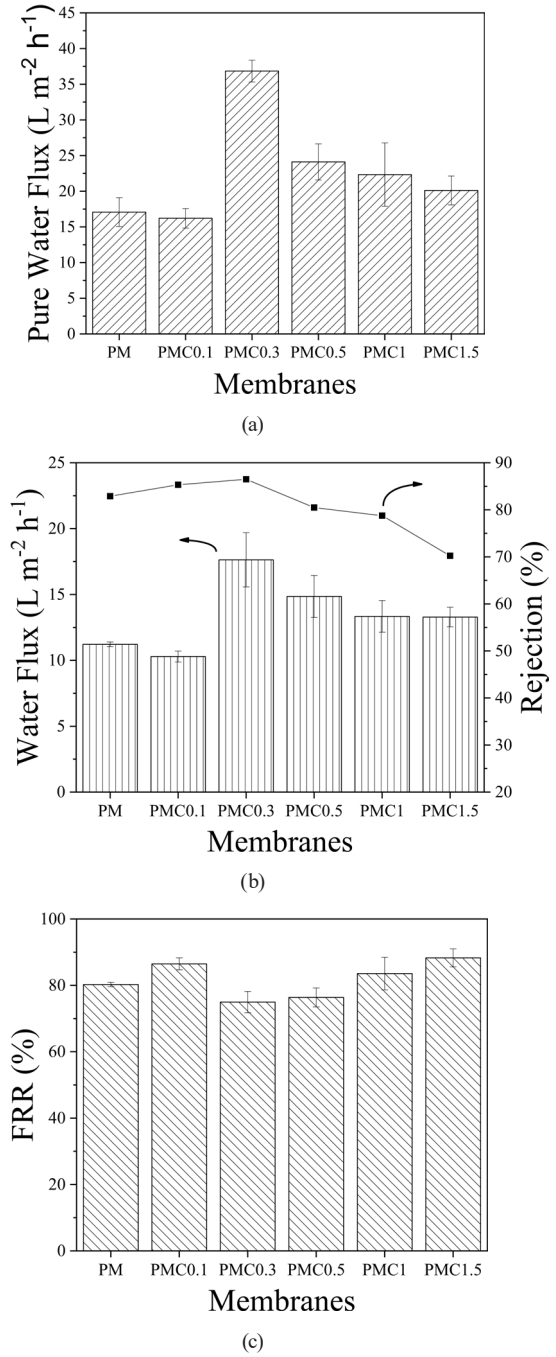

Fig. 4 Pure water flux (a), water flux and rejection (b), FRR (c) of PVDF and PVDF/SPC membranes

for all parameters examined was 4.93 in PMC1, indicating excellent homogeneity (SD < 5%). Cellulose addition significantly improved all PVDF membrane performances, such as PWF, water flux, rejection, and FRR ($p < 0.05$). Due to its superior performance compared to other membranes, PMC0.3 was further examined using SEM, ATR-FTIR, and TGA. Furthermore, 0.3% w/w addition of SPCB and SPCC were applied for PVDF membranes.

3.3 PVDF/SPCB and PVDF/SPCC

The PVDF/SPCB and PVDF/SPCC membranes has increased porosity and average pore size as a result of adding hydrophilic SPCB and SPCC (0.3% w/w) into PVDF matrix (Fig. 5 (a)). Presence of SPCB and SPCC accelerates the exchange rate between the solvent and non-solvent in phase inversion [7, 49]. With the addition of 0.3% w/w SPC, SPCB, and SPCC, the water contact angle of all fabricated PVDF membrane lowered (Fig. 5 (b)), indicating an increase in membrane hydrophilicity.

The PMCC0.3 membrane has the lowest water contact angle (75.5°), which potentially has better anti-fouling resistance [21]. The highest standard deviation (SD) obtained for all parameters examined was 4.82 in PMC0.3, indicating strong homogeneity (SD < 5%). The addition of all fillers significantly enhanced the PVDF membrane's porosity, average pore size, and water contact angle ($p < 0.05$).

PWF values of all modified PVDF membranes increased with addition of SPC, SPCB and SPCC (Fig. 6 (a)). The increased PWF value was in line with the increased porosity, where PMCB0.3 had the highest PWF value of

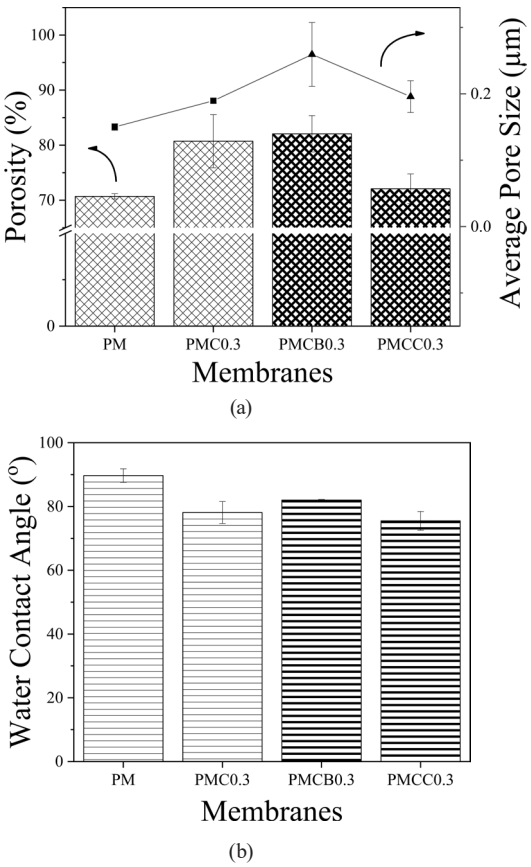

Fig. 5 Porosity and average pore size (a), water contact angle (b) of PVDF, PVDF/SPC, PVDF/SPCB and PVDF/SPCC membranes

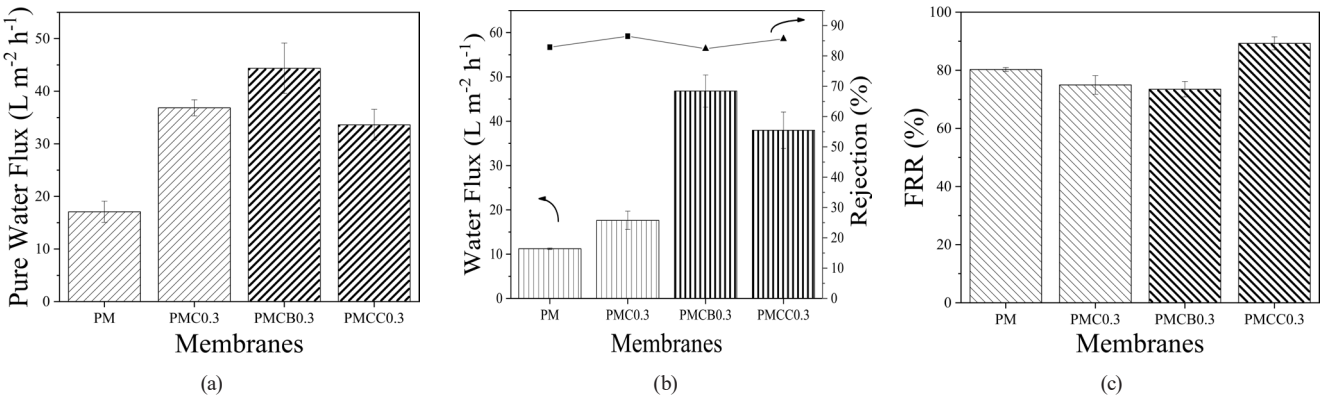

Fig. 6 Pure water flux (a), water flux and rejection (b), FRR (c) of PVDF, PVDF/SPC, PVDF/SPCB and PVDF/SPCC membranes

44.38 L m^{-2} h^{-1}. Interconnectivity of membrane pores resulted in highest PWF value, where water easily passed through the membrane [50, 51].

Water flux also affected water permeability. With the addition of fillers, the water flux values of PMC0.3, PMCB0.3, and PMCC0.3 increased (Fig. 6 (b)). PMCB0.3 membrane had the highest water flux value of 46.82 L m^{-2} h^{-1}. Water easily passes through the membrane as a result of the addition of hydrophilic fillers into PVDF matrix, which created larger pores and increased the rate of solvent and non-solvent exchange [7, 49, 52]. Otherwise, the larger pore may reduce the membranes' ability to reject contaminants [51].

In this study, PMCB0.3 membrane had the lowest rejection of MB, due to its high porosity which allowed MB molecules passed through the membranes (Fig. 6 (b)). Additionally, the rejection value for PMCC0.3 membrane was 85.64%, slightly less than the rejection rate for PMC 0.3, which was 86.50%. All modified PVDF membranes had good rejection values above 80%. PMC0.3 and PMCC 0.3 membranes have high rejection values as a result of the abundance of hydroxyl groups in cellulose and cellulose citrate that form hydrogen bonds with the $-NH_2$ group of MB [44].

The highest FRR value of 89.27% was obtained for PMCC0.3 membrane (Fig. 6 (c)). The highest hydrophilicity was also found for PMCC0.3 membrane, which increase its anti-fouling characteristics and reduced the hydrophobic contact between surface membrane and MB molecules [49]. For all parameter that we tested the highest standard deviation (SD) was obtained for porosity of 4.79 in PMCB0.3 which indicates good homogeneity (SD < 5%). All fillers addition increased PWF, water flux, and FRR significantly ($p < 0.05$) whereas it is insignificantly increased rejection ($p > 0.05$) of the PVDF membrane. Rejection and FRR are two parameters that are utilized on a commercial basis to assess membrane performances. Thus, PMCC0.3 was further examined by SEM, ATR-FTIR, and TGA since it had the best performance among PMC0.3 and PMCB0.3 membranes.

The surface and cross-section images of PM, PMC0.3, and PMCC0.3 membranes were shown in Fig. 7. All membranes had the asymmetric membrane characteristics of dense-skin layer, finger-like pore layer, and sponge-like pore layer. All membrane surfaces showed selective dense-skin layers that support membrane rejection [41]. Addition of SPC and SPCC formed longer finger-like structure than PVDF membrane, because hydroxyl groups enhanced the diffusional exchange rate of solvent and non-solvent in phase inversion [41, 43]. The longer finger-like structure confirmed that PMC0.3 and PMCC0.3 have higher PWF and water flux than PM membrane (Fig. 6 (a) and (b)).

The functional group in membrane surfaces was characterized using ATR-FTIR (Fig. 8 (a)). PMC0.3 and PMCC0.3 membranes have similar peaks to PM membrane. PVDF characteristic peaks are obtained in two vibrations. Vibrations of C-H symmetrical and asymmetric groups are shown at 3021 and 2980 cm^{-1}. Vibration of C-F group is shown at 1401, 1176, 1070 cm^{-1} [6]. Both peaks decreased the absorbance which indicated that cellulose and cellulose citrate successfully blended with PVDF and improve surface hydrophilicity of membrane. Cellulose and cellulose citrate absorption peaks of PMC0.3 and PMCC0.3 membranes show at 3337 and 2980 cm^{-1} for −OH group, and 2926 cm^{-1} for $-CH_2$ or $-CH_3$ group [6, 53]. Beta fraction values of PM, PMC0.3, and PMCC were similar, which were 0.3, 0.43, 0.46, and 0.44, respectively. The similar beta fraction value indicated that not all cellulose and cellulose citrate migrated to membrane surface.

PM, PMC0.3 and PMCC0.3 membranes have the similar thermal degradation that show in Fig. 8 (b). Initial weight loss less than 100 °C is evaporation of water content [54].

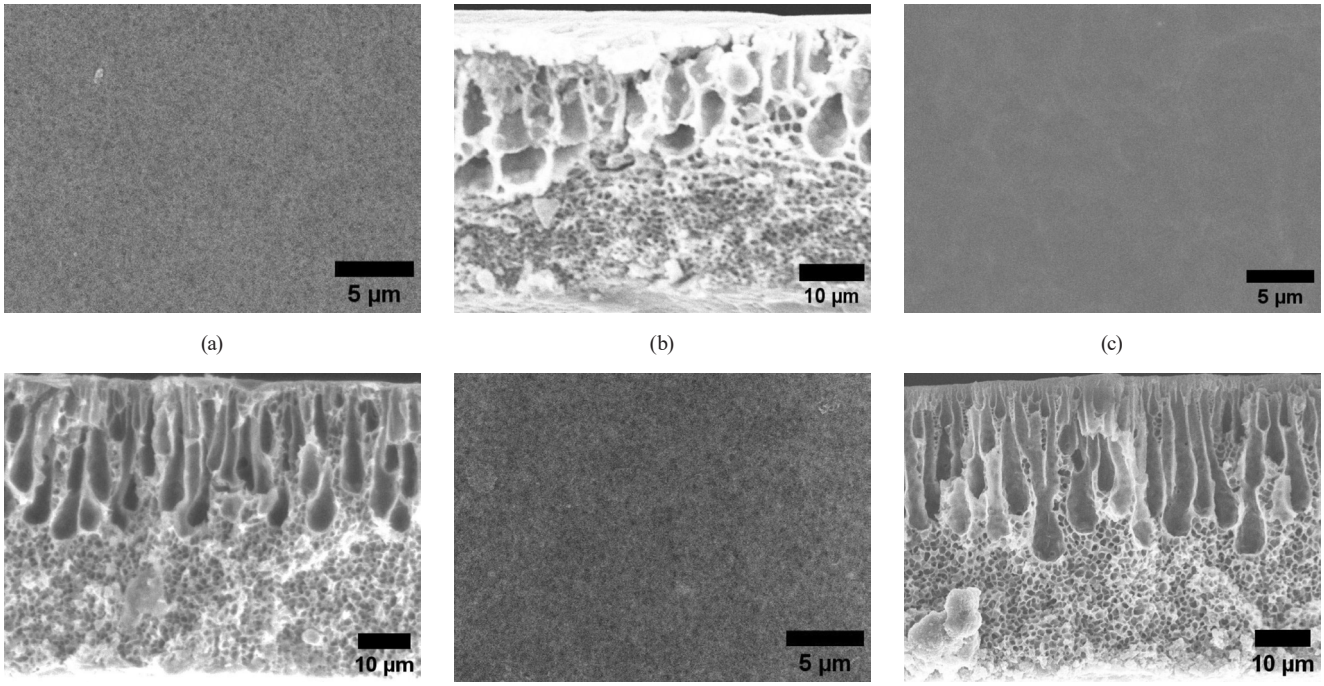

Fig. 7 SEM image of PM, PMC0.3, and PMCC0.3 surface (a, c, e) and cross-section (b, d, f) membranes

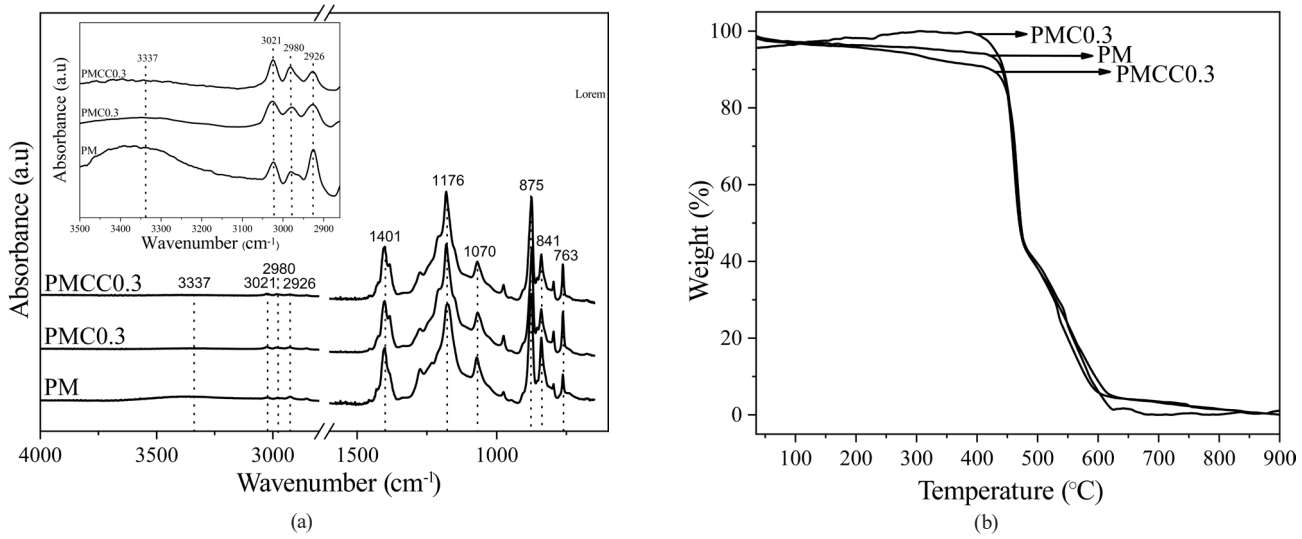

Fig. 8 ATR-FTIR spectra (a) and thermogram (b) of PM, PMC0.3 and PMCC0.3 membranes

PVDF polymer matrix degradation of PM, PMC0.3, and PMCC0.3 started at 440, 410, and 440 °C, respectively. All membrane had the similar temperature in second step degradation and last degradation at 510 °C and 620 °C, respectively. Thus, thermal stability of PVDF membranes was not significantly impacted by cellulose or cellulose citrate addition.

Rejection and FRR values of PMC0.3 and PMCC0.3 membranes were summarized in Table 2. In this study, the performance of PMC0.3 and PMCC0.3 membranes were better than PM membrane, while PMCB0.3 was comparable with PM membrane. Even at very low filler content in PVDF polymer could improve the membrane properties and performance [55]. In the same filtration method, PMC0.3, PMCB0.3, and PMCC0.3 have a better rejection of dye than modified PVDF membrane with GO/LiCl [4], Cu_2S nanoparticles [52], and Fe_3O_4@XG [1], also comparable with PVDF/-CD-HNTs [56]. This research revealed that cellulose, cellulose benzoate, and cellulose citrate screw pine leaves can be used as fillers for PVDF membrane which gave a comparable membrane performance with inorganic filler.

Table 2 The comparison study of rejection and FRR of MPC0.3 and MPCC0.3 with other studies

Filtration membrane	Filtration method	Feed	Rejection (%)	FRR (%)	References
PVDF	Dead-end	Methylene blue	82.89	80.26	This study
PMC0.3	Dead-end	Methylene blue	86.50	74.96	This study
PMCB0.3	Dead-end	Methylene blue	82.83	73.49	This study
PMCC0.3	Dead-end	Methylene blue	85.64	89.27	This study
PVDF/GO/LiCl	Dead-end	Rhodamine B	67.80	78.20	[4]
PVDF/-CD-HNTs	Dead-end	Direct red 28	88.10	88.30	[56]
PVDF/Cu_2S nanoparticles	Dead-end	Direct yellow 21	64.70	92.00	[52]
PVDF/Fe_3O_4@XG	Dead-end	Reactive red 120	~75.00	66.50	[1]

4 Conclusion

Cellulose benzoate and citrate were successfully synthesized from cellulose of screw pine (*Pandanus tectorius*) leaves by non-Fischer methods, which were confirmed by FT-IR spectra and thermogram TGA. Cellulose, cellulose benzoate, and cellulose citrate were used as fillers of PVDF membrane that was fabricated by blending-phase inversion method. Addition of 0.3% w/w cellulose and cellulose citrate into PVDF membrane improved hydrophilicity and membrane performance, such as water permeability, rejection, and anti-fouling properties. PVDF membrane has water flux value of 11.22 L m^{-2} h^{-1}, rejection value of 82.89%, and anti-fouling performance value of 80.26%. Addition of 0.35 w/w cellulose increased PVDF membrane water flux value to 17.63 L m^{-2} h^{-1} and rejection value to 86.50%, while decreased anti-fouling performance value to 74.96%. Addition 0.3% w/w of cellulose citrate increased all PVDF membrane performance, such as water flux value to 37.97%, rejection value to 85.64%, and anti-fouling properties to 89.27%. SEM images of PVDF modified with cellulose and cellulose citrate gave longer finger-like structure and smooth selective layer that improve the membrane performance. Generally, addition of 0.3% w/w cellulose and cellulose citrate into PVDF matrix improves the membrane performances. Cellulose addition increased all parameters significantly ($p < 0.05$), except for the porosity data, which increased insignificantly ($p > 0.05$). The addition of SPC0.3, SPCB0.3, and SPCC0.3 to PVDF membrane greatly improved all parameters ($p < 0.05$), although the only rejection data was insignificant ($p > 0.05$). Thus, the addition of SPC, SPCB, and SPCC should be performed to improve the characteristics and performance of PVDF membrane.

Acknowledgement

The authors thank to Universitas Sebelas Maret, Indonesia for financial support through research grants: 260/UN27.22/HK.07.00/2021; 254/27.22/PT.01.03/2022 and 469.1/UN27.22/PT.01.03/2022.

References

[1] Koyuncu, I., Yavuzturk Gul, B., Esmaeili, M. S., Pekgenc, E., Orhun Teber, O., Tuncay, G., Karimi, H., Parvaz, S., Maleki, A., Vatanpour, V. "Modification of PVDF membranes by incorporation Fe_3O_4@Xanthan gum to improve anti-fouling, anti-bacterial, and separation performance", Journal of Environmental Chemical Engineering, 10(3), 107784, 2022. https://doi.org/10.1016/j.jece.2022.107784

[2] Ahmad, H., Zahid, M., Rehan, Z. A., Rashid, A., Akram, S., Aljohani, M. M. H., Mustafa, S. K., Khalid, T., Abdelsalam, N. R., Ghareeb, R. Y., AL-Harbi, M. S. "Preparation of Polyvinylidene Fluoride Nano-Filtration Membranes Modified with Functionalized Graphene Oxide for Textile Dye Removal", Membranes, 12(2), 224, 2022. https://doi.org/10.3390/membranes12020224

[3] Mousavi, S. A., Arab Aboosadi, Z., Mansourizadeh, A., Honarvar, B. "Surface modified porous polyetherimide hollow fiber membrane for sweeping gas membrane distillation of dyeing wastewater", Colloids and Surfaces A: Physicochemical and Engineering Aspects, 610, 125439, 2021. https://doi.org/10.1016/j.colsurfa.2020.125439

[4] Zhu, Z., Wang, L., Xu, Y., Li, Q., Jiang, J., Wang, X. "Preparation and characteristics of graphene oxide-blending PVDF nanohybrid membranes and their applications for hazardous dye adsorption and rejection", Journal of Colloid and Interface Science, 504, pp. 429–439, 2017. https://doi.org/10.1016/j.jcis.2017.05.068

[5] Almaie, S., Vatanpour, V., Rasoulifard, M. H., Seyed Dorraji, M. S. "Novel negatively-charged amphiphilic copolymers of PVDF-g-PAMPS and PVDF-g-PAA to improve permeability and fouling resistance of PVDF UF membrane", Reactive and Functional Polymers, 179, 105386, 2022. https://doi.org/10.1016/j.reactfunctpolym.2022.105386

[6] Lv, J., Zhang, G., Zhang, H., Zhao, C., Yang, F. "Improvement of antifouling performances for modified PVDF ultrafiltration membrane with hydrophilic cellulose nanocrystal", Applied Surface Science, 440, pp. 1091–1100, 2018. https://doi.org/10.1016/j.apsusc.2018.01.256

[7] Tan, H.-F., Tan, W.-L., Ooi, B. S., Leo, C. P. "Superhydrophobic PVDF/micro fibrillated cellulose membrane for membrane distillation crystallization of struvite", Chemical Engineering Research and Design, 170, pp. 54–68, 2021.
https://doi.org/10.1016/j.cherd.2021.03.027

[8] Muqeet, M., Mahar, R. B., Gadhi, T. A., Ben Halima, N. "Insight into cellulose-based-nanomaterials - A pursuit of environmental remedies", International Journal of Biological Macromolecules, 163, pp. 1480–1486, 2020.
https://doi.org/10.1016/j.ijbiomac.2020.08.050

[9] Aziz, T., Farid, A., Haq, F., Kiran, M., Ullah, A., Zhang, K., Li, C., Ghazanfar, S., Sun, H., Ullah, R., Ali, A., … Al Jaouni, S. K. "A Review on the Modification of Cellulose and Its Applications", Polymers, 14(15), 3206, 2022.
https://doi.org/10.3390/polym14153206

[10] Akinjokun, A. I., Petrik, L. F., Ogunfowokan, A. O., Ajao, J., Ojumu, T. V. "Isolation and characterization of nanocrystalline cellulose from cocoa pod husk (CPH) biomass wastes", Heliyon, 7(4), e06680, 2021.
https://doi.org/10.1016/j.heliyon.2021.e06680

[11] Nurhaliza, Y., Nurulhaq, F., Yudhanto, S. M., Suryanti, V. "Edible film from microcrystalline cellulose (MCC) of waste banana (*Musa paradisiaca*) stem and chitosan", Journal of Physics: Conference Series, 2190, 012027, 2022.
https://doi.org/10.1088/1742-6596/2190/1/012027

[12] Bano, S., Negi, Y. S. "Studies on cellulose nanocrystals isolated from groundnut shells", Carbohydrate Polymers, 157, pp. 1041–1049, 2017.
https://doi.org/10.1016/j.carbpol.2016.10.069

[13] Candido, R. G., Godoy, G. G., Gonçalves, A. R. "Characterization and application of cellulose acetate synthesized from sugarcane bagasse", Carbohydrate Polymers, 167, pp. 280–289, 2017.
https://doi.org/10.1016/j.carbpol.2017.03.057

[14] Jebadurai, S. G., Raj, R. D. E., Sreenivasan, V. S., Binoj, J. S. "Coccinia grandis stem fiber polymer composite: thermal and mechanical analysis", Iranian Polymer Journal, 30(4), pp. 369–380, 2021.
https://doi.org/10.1007/s13726-020-00896-4

[15] Afolabi, L. O., Megat-Yusoff, P. S. M., Ariff, Z. M., Hamizol, M. S. "Fabrication of pandanus tectorius (screw-pine) natural fiber using vacuum resin infusion for polymer composite application", Journal of Materials Research and Technology, 8(3), pp. 3102–3113, 2019.
https://doi.org/10.1016/j.jmrt.2017.05.021

[16] Sheltami, R. M., Abdullah, I., Ahmad, I., Dufresne, A., Kargarzadeh, H. "Extraction of cellulose nanocrystals from mengkuang leaves (*Pandanus tectorius*)", Carbohydrate Polymers, 88(2), pp. 772–779, 2012.
https://doi.org/10.1016/j.carbpol.2012.01.062

[17] Wsoo, M. A., Shahir, S., Mohd Bohari, S. P., Nayan, N. H. M., Razak, S. I. A. "A review on the properties of electrospun cellulose acetate and its application in drug delivery systems: A new perspective", Carbohydrate Research, 491, 107978, 2020.
https://doi.org/10.1016/j.carres.2020.107978

[18] Zhao, X., Anwar, I., Zhang, X., Pellicciotti, A., Storts, S., Nagib, D. A., Vodovotz, Y. "Thermal and Barrier Characterizations of Cellulose Esters with Variable Side-Chain Lengths and Their Effect on PHBV and PLA Bioplastic Film Properties", ACS Omega, 6(38), pp. 24700–24708, 2021.
https://doi.org/10.1021/acsomega.1c03446

[19] Hossein Razzaghi, M., Safekordi, A., Tavakolmoghadam, M., Rekabdar, F., Hemmati, M. "Morphological and separation performance study of PVDF/CA blend membranes", Journal of Membrane Science, 470, pp. 547–557, 2014.
https://doi.org/10.1016/j.memsci.2014.07.026

[20] Mu, C., Su, Y., Sun, M., Chen, W., Jiang, Z. "Remarkable improvement of the performance of poly(vinylidene fluoride) microfiltration membranes by the additive of cellulose acetate", Journal of Membrane Science, 350(1–2), pp. 293–300, 2010.
https://doi.org/10.1016/j.memsci.2010.01.004

[21] Pramono, E., Zakaria, M. A., Fridiasari, K. F., Ndruru, S. T. C. L., Bagaskara, M., Mustofa, R. E., Sejati, G. P. W., Purnawan, C., Saputra, O. A. "Cellulose derived from oil palm empty fruit bunches as filler on polyvinylidene fluoride based membrane for water containing humic acid treatment", Groundwater for Sustainable Development, 17, 100744, 2022.
https://doi.org/10.1016/j.gsd.2022.100744

[22] Cheng, J., Zhan, C., Wu, J., Cui, Z., Si, J., Wang, Q., Peng, X., Turng, L.-S. "Highly Efficient Removal of Methylene Blue Dye from an Aqueous Solution Using Cellulose Acetate Nanofibrous Membranes Modified by Polydopamine", ACS Omega, 5(10), pp. 5389–5400, 2020.
https://doi.org/10.1021/acsomega.9b04425

[23] Lv, J., Zhang, G., Zhang, H., Yang, F. "Exploration of permeability and antifouling performance on modified cellulose acetate ultrafiltration membrane with cellulose nanocrystals", Carbohydrate Polymers, 174, pp. 190–199, 2017.
https://doi.org/10.1016/j.carbpol.2017.06.064

[24] Silva, M. A., Belmonte-Reche, E., de Amorim, M. T. P. "Morphology and water flux of produced cellulose acetate membranes reinforced by the design of experiments (DOE)", Carbohydrate Polymers, 254, 117407, 2021.
https://doi.org/10.1016/j.carbpol.2020.117407

[25] Li, Y., Hu, Q., Zhang, R., Ma, W., Pan, S., Zhao, Y., Wang, Q., Fang, P. "Piezoelectric Nanogenerator Based on Electrospinning PVDF/Cellulose Acetate Composite Membranes for Energy Harvesting", Materials, 15(19), 7026, 2022.
https://doi.org/10.3390/ma15197026

[26] Peluso, P., Mamane, V., Dallocchio, R., Dessì, A., Cossu, S. "Noncovalent interactions in high-performance liquid chromatography enantioseparations on polysaccharide-based chiral selectors", Journal of Chromatography A, 1623, 461202, 2020.
https://doi.org/10.1016/j.chroma.2020.461202

[27] Zhou, Y., Zhang, X., Cheng, Y., Zhang, J., Mi, Q., Yin, C., Wu, J., Zhang, J. "Super-rapid and highly-efficient esterification of cellulose to achieve an accurate chromatographic analysis of its molecular weight", Carbohydrate Polymers, 286, 119301, 2022.
https://doi.org/10.1016/j.carbpol.2022.119301

[28] Olivito, F., Algieri, V., Jiritano, A., Tallarida, M. A., Tursi, A., Costanzo, P., Maiuolo, L., De Nino, A. "Cellulose citrate: A convenient and reusable bio-adsorbent for effective removal of methylene blue dye from artificially contaminated water", RSC Advances, 11(54), pp. 34309–34318, 2021.
https://doi.org/10.1039/d1ra05464c

[29] Sridevi, S., Sutha, S., Kavitha, L., Gopi, D. "Valorization of biowaste derived nanophase yttrium substituted hydroxyapatite/ citrate cellulose/ *opuntia* mucilage biocomposite: A template assisted synthesis for potential biomedical applications", Materials Chemistry and Physics, 273, 125144, 2021.
https://doi.org/10.1016/j.matchemphys.2021.125144

[30] Tursi, A., Gallizzi, V., Olivito, F., Algieri, V., De Nino, A., Maiuolo, L., Beneduci, A. "Selective and efficient mercury(II) removal from water by adsorption with a cellulose citrate biopolymer", Journal of Hazardous Materials Letters, 3, 100060, 2022.
https://doi.org/10.1016/j.hazl.2022.100060

[31] Punnadiyil, R. K., Sreejith, M. P., Purushothaman, E. "Isolation of microcrystalline and nano cellulose from peanut shells", Journal of Chemical and Pharmaceutical Sciences, 2016, pp. 12–16, 2016.

[32] Zhang, J., Wu, J., Cao, Y., Sang, S., Zhang, J., He, J. "Synthesis of cellulose benzoates under homogeneous conditions in an ionic liquid", Cellulose, 16(2), pp. 299–308, 2009.
https://doi.org/10.1007/s10570-008-9260-2

[33] Solo, A. A. M., Masruri, M., Rumhayati, B. "Characteristic of cellulose isolated from papyrus fibers (Borrasus flabelifer L) and its citrate ester", The Journal of Pure and Applied Chemistry Research, 7(3), pp. 239–246, 2018.
https://doi.org/10.21776/ub.jpacr.2018.007.03.410

[34] Wang, Y., Wang, X., Xie, Y., Zhang, K. "Functional nanomaterials through esterification of cellulose: a review of chemistry and application", Cellulose, 25(7), pp. 3703–3731, 2018.
https://doi.org/10.1007/s10570-018-1830-3

[35] Fei, P., Liao, L., Cheng, B., Song, J. "Quantitative analysis of cellulose acetate with a high degree of substitution by FTIR and its application", Analytical Methods, 9(43), pp. 6194–6201, 2017.
https://doi.org/10.1039/C7AY02165H

[36] Cui, X., Honda, T., Asoh, T.-A., Uyama, H. "Cellulose modified by citric acid reinforced polypropylene resin as fillers", Carbohydrate Polymers, 230, 115662, 2020.
https://doi.org/10.1016/j.carbpol.2019.115662

[37] Chen, J., Xu, J., Wang, K., Cao, X., Sun, R. "Cellulose acetate fibers prepared from different raw materials with rapid synthesis method", Carbohydrate Polymers, 137, pp. 685–692, 2016.
https://doi.org/10.1016/j.carbpol.2015.11.034

[38] Spinella, S., Maiorana, A., Qian, Q., Dawson, N. J., Hepworth, V., McCallum, S. A., Ganesh, M., Singer, K. D., Gross, R. A. "Concurrent Cellulose Hydrolysis and Esterification to Prepare a Surface-Modified Cellulose Nanocrystal Decorated with Carboxylic Acid Moieties", ACS Sustainable Chemistry & Engineering, 4(3), pp. 1538–1550, 2016.
https://doi.org/10.1021/acssuschemeng.5b01489

[39] Huang, F., Wu, X., Yu, Y., Lu, Y., Chen, Q. "Acylation of cellulose nanocrystals with acids/trifluoroacetic anhydride and properties of films from esters of CNCs", Carbohydrate Polymers, 155, pp. 525–534, 2017.
https://doi.org/10.1016/j.carbpol.2016.09.010

[40] Sun, Z., Wang, P., Lu, D., Liu, C., Ma, J. "Synergistic effects of matrix-anchoring and surface-segregation behavior of poly(N-vinylpyrrolidone)-grafted-silica filler for PVDF membrane performance improvement", Separation and Purification Technology, 276, 119353, 2021.
https://doi.org/10.1016/j.seppur.2021.119353

[41] Gholami, S., Llacuna, J. L., Vatanpour, V., Dehqan, A., Paziresh, S., Cortina, J. L. "Impact of a new functionalization of multi-walled carbon nanotubes on antifouling and permeability of PVDF nanocomposite membranes for dye wastewater treatment", Chemosphere, 294, 133699, 2022.
https://doi.org/10.1016/j.chemosphere.2022.133699

[42] Dlamini, D. S., Matindi, C., Vilakati, G. D., Tesha, J. M., Motsa, M. M., Thwala, J. M., Mamba, B. B., Hoek, E. M. V., Li, J. "Fine-tuning the architecture of loose nanofiltration membrane for improved water flux, dye rejection and dye/salt selective separation", Journal of Membrane Science, 621, 118930, 2021.
https://doi.org/10.1016/j.memsci.2020.118930

[43] Nazri, A. I., Ahmad, A. L., Hussin, M. H. "Microcrystalline Cellulose-Blended Polyethersulfone Membranes for Enhanced Water Permeability and Humic Acid Removal", Membranes, 11(9), 660, 2021.
https://doi.org/10.3390/membranes11090660

[44] Oyarce, E., Butter, B., Santander, P., Sánchez, J. "Polyelectrolytes applied to remove methylene blue and methyl orange dyes from water via polymer-enhanced ultrafiltration", Journal of Environmental Chemical Engineering, 9(6), 106297, 2021.
https://doi.org/10.1016/j.jece.2021.106297

[45] Bendoy, A. P., Zeweldi, H. G., Park, M. J., Shon, H. K., Kim, H., Chung, W.-J., Nisola, G. M. "Silicene nanosheets as support fillers for thin film composite forward osmosis membranes", Desalination, 536, 115817, 2022.
https://doi.org/10.1016/j.desal.2022.115817

[46] Bangari, R. S., Yadav, A., Bharadwaj, J., Sinha, N. "Boron nitride nanosheets incorporated polyvinylidene fluoride mixed matrix membranes for removal of methylene blue from aqueous stream", Journal of Environmental Chemical Engineering, 10(1), 107052, 2022.
https://doi.org/10.1016/j.jece.2021.107052

[47] Nawaz, H., Umar, M., Ullah, A., Razzaq, H., Zia, K. M., Liu, X. "Polyvinylidene fluoride nanocomposite super hydrophilic membrane integrated with Polyaniline-Graphene oxide nano fillers for treatment of textile effluents", Journal of Hazardous Materials, 403, 123587, 2021.
https://doi.org/10.1016/j.jhazmat.2020.123587

[48] Thooyavan, Y., Kumaraswamidhas, L. A., Raj, R. D. E., Binoj, J. S., Brailson Mansingh, B. "Effect of combined micro and nano silicon carbide particles addition on mechanical, wear and moisture absorption features of basalt bidirectional mat/vinyl ester composites", Polymer Composites, 43(5), pp. 2574–2583, 2022. https://doi.org/10.1002/pc.26557

[49] Ayyaru, S., Dinh, T. T. L., Ahn, Y.-H. "Enhanced antifouling performance of PVDF ultrafiltration membrane by blending zinc oxide with support of graphene oxide nanoparticle", Chemosphere, 241, 125068, 2020. https://doi.org/10.1016/j.chemosphere.2019.125068

[50] Rabiee, H., Vatanpour, V., Farahani, M. H. D. A., Zarrabi, H. "Improvement in flux and antifouling properties of PVC ultrafiltration membranes by incorporation of zinc oxide (ZnO) nanoparticles", Separation and Purification Technology, 156, pp. 299–310, 2015. https://doi.org/10.1016/j.seppur.2015.10.015

[51] Jiang, C., Tian, L., Hou, Y., Niu, Q. J. "Nanofiltration membranes with enhanced microporosity and inner-pore interconnectivity for water treatment: Excellent balance between permeability and selectivity", Journal of Membrane Science, 586, pp. 192–201, 2019. https://doi.org/10.1016/j.memsci.2019.05.075

[52] Karimi, A., Khataee, A., Ghadimi, A., Vatanpour, V. "Ball-milled Cu_2S nanoparticles as an efficient additive for modification of the PVDF ultrafiltration membranes: Application to separation of protein and dyes", Journal of Environmental Chemical Engineering, 9(2), 105115, 2021. https://doi.org/10.1016/j.jece.2021.105115

[53] Makanjuola, O., Ahmed, F., Janajreh, I., Hashaikeh, R. "Development of a dual-layered PVDF-HFP/cellulose membrane with dual wettability for desalination of oily wastewater", Journal of Membrane Science, 570–571, pp. 418–426, 2019. https://doi.org/10.1016/j.memsci.2018.10.028

[54] Nasr, R. A., Ali, E. A. "Polyethersulfone/gelatin nano-membranes for the Rhodamine B dye removal and textile industry effluents treatment under cost effective condition", Journal of Environmental Chemical Engineering, 10(2), 107250, 2022. https://doi.org/10.1016/j.jece.2022.107250

[55] Karthik, K., Prakash, J. U., Binoj, J. S., Mansingh, B. B. "Effect of stacking sequence and silicon carbide nanoparticles on properties of carbon/glass/Kevlar fiber reinforced hybrid polymer composites", Polymer Composites, 43(9), pp. 6069–6105, 2022. https://doi.org/10.1002/pc.26912

[56] Ma, J., He, Y., Zeng, G., Yang, X., Chen, X., Zhou, L., Peng, L., Sengupta, A. "High-flux PVDF membrane incorporated with β-cyclodextrin modified halloysite nanotubes for dye rejection and Cu (II) removal from water", Polymers for Advanced Technologies, 29(11), pp. 2704–2714, 2018. https://doi.org/10.1002/pat.4356